Experimental Tests of Two-Phase Fluid Model of Drying Consolidation

L. A. Brown and C. F. Zukoski
Dept. of Chemical Engineering, University of Illinois at Urbana-Champaign, Urbana, IL 61801

Drying of aggregated slurries proceeds through a stage of consolidation prior to bed desaturation. During this period, volume fraction profiles develop within the bed. The magnitude of volume fraction variation is controlled by the rate of mass transfer and the strength of the bed. A two-phase fluid model for stress balances in conjunction with the compressive yield stress constitutive equation is explored to describe the temporal evolution of bed volume fraction profiles. For this purpose, the compressive rheology of the saturated bed is characterized through independent experiments that fix all adjustable parameters. Excellent agreement is found between model predictions and experimental results.

Introduction

The process of separation of suspensions of particles into their component solid and liquid portions occur in a wide range of technologies. The specific separation technique employed varies greatly and depends on a number of factors including the suspension's solids content, the desired rate of separation, the degree of separation required, and the overall cost of the process. Common separation techniques employed for supensions included pressure filtration, sedimentation, and drying.

Two-phase models have been developed to describe solid-liquid separation of compressible slurries (Tiller and Hsyung, 1993; Buscall and White, 1987). These models require a constitutive equation relating deformation to applied load. Buscall and White (1987) proposed a constitutive model for the rate of volume fraction change in the presence of a compressive load that employs a volume fraction dependent compressive yield stress $P_y(\phi)$. For loads less than $P_y(\phi)$, the bed responds elastically, while for compressive loads larger than $Py(\phi)$, the bed consolidates. The constitutive equation was developed by Buscall and White (1987) and is written as

$$\frac{D\phi}{Dt} = 0; \qquad P_s < P_y(\phi)$$

$$\frac{D\phi}{Dt} = \kappa(\phi)\left[P_s - P_y(\phi)\right] \qquad P_s \geq P_y(\phi) \qquad (1)$$

where P_s is the load acting on the particulate phase through direct particle interaction forces, ϕ is the volume fraction, and $\kappa(\phi)$ is the dynamic compressibility. Under conditions where the lefthand side of Eq. 1 is of order unity, Buscall and White (1987) argue that $\kappa(\phi)$ is large and $P_s \approx P_y$ at all points in the suspension. This approximation greatly simplifies analysis of the compressive rheology of aggregated slurries.

The compressive yield stress constitutive equation is used increasingly in predictions of pressure filter performance, in thick bed settler design, and in slurry drying (Landman et al., 1988, 1991; Brown et al., 2002). The ability of this constitutive equation to capture compressive behavior of aggregated slurries has been tested primarily by demonstrating that $P_y(\phi)$ is independent of the method by which the compressive load is applied. The same values, for example, of $P_y(\phi)$ are measured by pressure filtration, sedimentation, centrifugal loading, and osmotic consolidation (Green et al., 1996; Miller et al., 1996; Green and Boger, 1997; Usher et al., 2001). Dynamic tests are primarily limited to demonstrating that, under constant loads in a pressure filter, the volume of expressed fluid increases as $t^{1/2}$, where t is the filtration time. This result is insensitive to the constitutive equations used to describe slurry consolidation (Landman et al., 1995; Sherwood and Meeten, 1997). As such, confirmation of the $t^{1/2}$ behavior is not a very severe test of the constitutive equation used.

More recently, a two-phase fluid model incorporating Eq. 1 was developed for the early stages of drying of saturated beds (Brown et al., 2002). The two-phase fluid approach links the rate of consolidation to the rate of the continuous or liquid phase escapes from the slurry. For saturated bodies, the rate at which mass leaves is controlled by the mass-transfer coefficient k_g. While the slurry remains saturated, the bed

Correspondence concerning this article should be addressed to C. F. Zukoski.

must consolidate in response to this loss of fluid. The model characterizes the strength of the bed through the compressive yield stress constitutive equation, such that from knowledge of k_g and $P_y(\phi)$, volume fraction profiles can be predicted. High drying rates result in very steep volume fraction profiles, while slow drying results in consolidation with essentially uniform volume fraction profiles. The relative rates of drying and consolidation are characterized by the dimensionless group $\overline{Q} = k_g h_0/D(\phi)$, where h_0 is the characteristic bed thickness and $D(\phi)$ is the filtration diffusivity $D(\phi)$ that explicitly depends on bed permeability and $P_y(\phi)$.

The consolidation period of drying ends when the drying body begins to desaturate. This occurs when the capillary forces acting within the pores of the body approach the maximum capillary pressure $P_{\text{cap}}^{\max}$ that the liquid can apply to the bed. $P_{\text{cap}}^{\max}$ is the capillary pressure that would exist if the saturated bed were allowed to equilibrate with the gas phase with no changes in volume fraction. This equilibrium or maximum capillary pressure is a weak function of volume fraction. As long as $P_{\text{cap}}^{\max}(\phi) > P_y(\phi)$, the body will consolidate. However, $P_y(\phi)$ increases rapidly with ϕ such that, when $\phi = \phi_e$, $P_y(\phi_e) = P_{\text{cap}}^{\max}(\phi_e)$. For drying times $t > t_e$, the bed begins to desaturate. Here, t_e is the drying time required for the volume fraction at the edges of the drying body to reach ϕ_e. For aggregated slurries consisting of particles with poorly characterized particle size, shape, and packing characteristics, the capillary forces are difficult to characterize in an *a priori* manner. As with the permeability of aggregated slurries, $P_{\text{cap}}^{\max}(\phi)$ must be experimentally characterized to accurately predict drying rates and shape changes during drying.

Detailed tests of the two-phase model and compressive yield stress constitutive equation require that the time and rate of change of volume fraction be measured. In this article we characterize the compressive properties of aggregated suspensions through measurement of $P_y(\phi)$. By measuring the rate of filtration under a constant load, estimates of $D(\phi)$ are made. These parameters are then employed with no further adjustments to predict the evolution of volume fraction profiles in compressible drying beds. This use of parameters, measured using one mechanism of consolidation to predict $\phi(z, t)$ in a bed being compressed in an independent process, provides a rigorous test of the compressive yield stress constitutive model.

In the next section we develop the basic methods by which $P_y(\phi)$ and $D(\phi)$ are characterized and provide a summary of the drying model. The experimental techniques employed are described, followed by a discussion of the experimental results and a comparison with model predictions. Finally, conclusions are drawn.

Two-Phase Model Development

Assuming negligible variation in a volume fraction across a cylinder containing a compressible suspension, as depicted in Figure 1a, Landman and Russel (1993) developed force balances on the particulate and fluid phases as follows:

For the particulate phase

$$\frac{\partial P_s}{\partial z} + \frac{\eta\phi R(\phi)}{a_p^2}(u - v) + \Delta\rho g\phi = 0 \qquad (2)$$

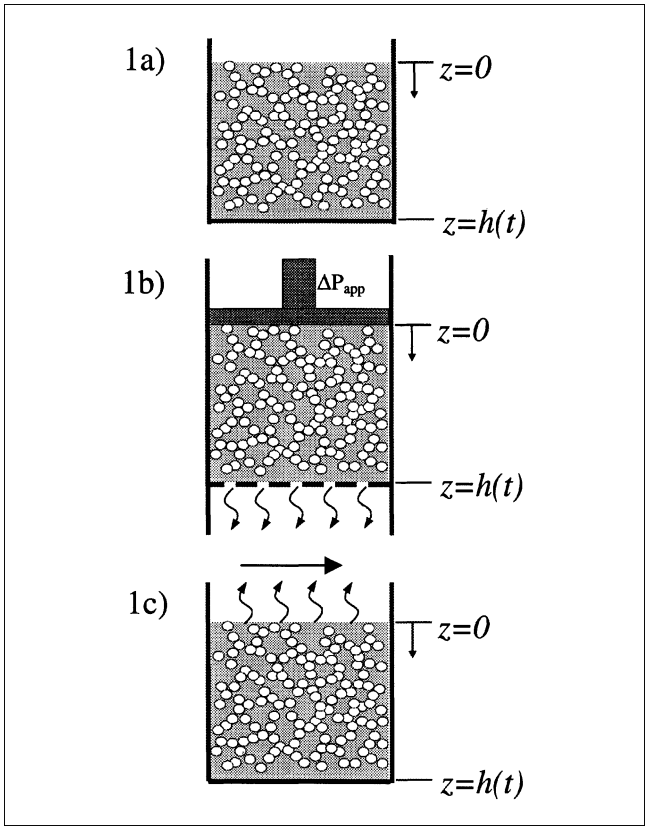

Figure 1. Aggregated suspension.

(a) In cylinder; (b) in pressure filter; and (c) in drying.

For the fluid phase

$$\frac{\partial P_l}{\partial z} + \frac{\eta\phi R(\phi)}{a_p^2}(v - u) + \rho_f g = 0 \qquad (3)$$

where P_s and P_l are the particulate and fluid pressures, respectively, η is the fluid viscosity, a_p is the characteristic particle radius, u and v are the particulate and fluid velocities, respectively, $\Delta\rho = \rho_s - \rho_f$ is the difference between the particulate and fluid densities, g is the gravitational acceleration, and $R(\phi)$ accounts for hydrodynamic interactions between particles as they move through the suspending fluid. Taken with Eq. 1 and continuity equations for conservation of fluid and solid mass, balance Eqs. 2 and 3 represent a closed description of the time and position dependence of the volume fraction, fluid and solid velocities, and fluid and solid pressures.

By assuming that $\kappa(\phi)$ is large in Eq. 1, Buscall and White (1987) concluded that under a consolidating load, $P_y(\phi) \approx P_s(\phi)$ allowing dP_s/dz in Eq. 2 to be rewritten as $dP_y/d\phi\, d\phi/dz$. This simplifaction can be used in conjunction with Eq. 2 to develop experimental methods for detemining $P_y(\phi)$. In constant pressure filtration a compressive load is applied to the suspension, as shown in Figure 1b with the fluid being allowed to leave via a semi-permeable membrane. If gravitational forces are negligible relative to the applied load, then adding Eqs. 2 and 3 and integrating the result yields $P_s + P_l = P_{\text{app}}$, where P_{app} is the applied pressure. If u and v are

zero (that is, the end of filtration when steady state is reached), the liquid does not support the applied load so that $P_l = 0$ and $P_s = P_{app}$. The volume fraction ϕ is measured at time t_f when there are no further changes in the height of the suspension. As $t \to t_f$, $\phi \to \phi(t_f)$ for all z. This result has been confirmed experimentally (Miller et al., 1996; Yoon, 2000). Thus, if a series of pressures is applied and $\phi(t_f)$ measured for each pressure, $P_y(\phi)$ can be determined.

Similar arguments are used for a centrifuge experiment where a bed is consolidated under its own weight and the volume fraction profile determined (Miller et al., 1996; Green et al., 1996). There, from knowledge of $\phi(z)$, particle and fluid densities, as well as gravitational acceleration, $P_y(\phi)$ can be determined (Buscall and McGowan, 1983; Auzerais et al., 1988; Bergström et al., 1992; Miller et al., 1996; Green et al., 1996). If a suspension is centrifuged until the bed reaches a steady-state height, the stress acting on the particles is obtained at steady state by integrating Eq. 2 as

$$P_y(\phi(z)) = \Delta\rho\omega^2 \int_0^z s\phi(s)ds \tag{4}$$

where $\Delta\rho$ is the difference between the particle and fluid densities, ω is the angular velocity, and $g = \omega^2 z$. Thus, from a knowledge of the $\phi(z)$ in the bed, $P_y(\phi)$ can be determined. We use below both pressure filtration and centrifugation to characterize $P_y(\phi)$.

Bed characterization with constant pressure filtration

To characterize the dynamics of consolidation, we rewrite Eq. 2 as

$$\frac{a_p^2}{\eta R(\phi)} \frac{\partial P_y}{\partial \phi} \frac{\partial \phi}{\partial z} + \phi(u - v) = 0 \tag{5}$$

where we have assumed gravitational forces are negligible (that is, $\Delta\rho g\phi/P_y(\phi) \ll 1$). In order to eliminate the fluid velocity, v from Eq. 5, we utilize the equations of continuity that are required for conservation of mass in the system

$$\frac{\partial \phi}{\partial t} + \frac{\partial(\phi u)}{\partial z} = 0 \tag{6}$$

$$\frac{\partial(1-\phi)}{\partial t} + \frac{\partial[(1-\phi)v]}{\partial z} = 0 \tag{7}$$

We use a coordinate system shown in Figure 1 where the particles and fluid at $z = 0$ move at the same rate as the surface of the piston given by $u = v = -dh/dt$. With this boundary condition, Eqs. 6 and 7 can be solved to yield

$$\phi u + (1-\phi)v = -\frac{dh}{dt} \tag{8}$$

Solving for v in Eq. 8 and substituting into Eq. 5 yields

$$D(\phi)\frac{\partial \phi}{\partial z} = \phi\left(u + \frac{dh}{dt}\right) \tag{9}$$

where

$$D(\phi) = \frac{a_p^2(1-\phi)}{\eta R(\phi)} \frac{\partial P_y}{\partial \phi} \tag{10}$$

is the filtration diffusivity. Note that the filtration diffusivity $D(\phi)$ contains material properties that can be determined independently of the particular consolidation experiment being modeled. The filtration diffusivity involves $dP_y/d\phi$ and bed hydrodynamic resistance $R(\phi)$, or equivalently the bed permeability $k(\phi)$, where

$$k(\phi) = \frac{a_p^2(1-\phi)}{\phi R(\phi)} \tag{11}$$

As beds may be composed of aggregated particles with potentially broad size and shape distributions, $k(\phi)$ is not known *a priori*. As a result, methods for measuring $D(\phi)$ or $k(\phi)$ have been developed. One of the easiest to implement for compressible beds is based on the empirical observation that the volume of filtrate expressed per unit of filter cross-section is often well approximated by

$$H = \beta\sqrt{t} \tag{12}$$

where t is filtration time and β is a constant that can be determined from a straight line plot of t/H vs. H which has slope β^2. Landman et al. (1999) demonstrate that when Eq. 12 is satisfied, an approximate relation between β and $D(\phi)$ is

$$D(\phi_\infty) = \frac{d\beta^2/d\phi_\infty}{2\left(\frac{1}{\phi_0} - \frac{1}{\phi_\infty}\right)} \tag{13}$$

where ϕ_0 is the initial volume fraction and ϕ_∞ is the equilibrium volume fraction after consolidation. Alternately, we can obtain $R(\phi)$ directly using Eq. 10 as

$$R(\phi_\infty) = \frac{2a_p^2\left(\frac{1}{\phi_0} - \frac{1}{\phi_\infty}\right)(1-\phi_\infty)}{\eta\frac{d\beta^2}{d\Delta P}} \tag{14}$$

where ΔP is the applied compressive load. Thus, from a series of constant pressure filtration experiments, both $P_y(\phi)$ and $D(\phi)$ can be extracted.

Descriptions of consolidation kinetics are made by combining Eqs. 6 and 9 to yield

$$\frac{\partial \phi}{\partial t} = \frac{\partial}{\partial z}\left(D(\phi)\frac{\partial \phi}{\partial z} + \phi Q\right) \tag{15}$$

where $Q = -dh/dt$ is the rate at which the bed height $h(t)$ collapses. Equation 15 governs the dynamics of the consolidation process and can be solved with initial and boundary conditions specific to a given consolidation method.

For constant pressure filtration, we assume an initially constant volume fraction such that

$$\phi(z,0) = \phi_0 \qquad 0 \le z \le h_0 \tag{16}$$

where h_0 is the initial height of the suspension. At the filter membrane, the boundary condition is obtained by matching the flux of liquid out of the membrane with the flux of liquid to the membrane from the bed (Landman et al., 1991). This yields a boundary condition that can be expressed as

$$P_y - R_f \frac{\partial P_y}{\partial z} = P_{\text{app}} \tag{17}$$

where R_f is the resistance of the filter membrane. When the resistance of the membrane is negligible, Eq. 17 reduces to $P_y(\phi) = P_{\text{app}}$, which sets the volume fraction at the membrane. At the piston/suspension interface, a no flux condition prevails yielding

$$\left.\frac{\partial \phi}{\partial z}\right|_{(h(t),t)} = 0 \qquad t \ge 0 \tag{18}$$

Given $P_y(\phi)$, $D(\phi)$, and Eqs. 15–18, $\phi(z,t)$ and $h(t)$ can be determined. Below, we demonstrate the ability of this model to capture $h(t)$ at different P_{app}.

Drying kinetics

In applying this two-phase fluid model to the initial stages of drying, we start by considering a saturated suspension that has formed a space-filling network of initially uniform volume fraction, as shown in Figure 1c. As with pressure filtration, the initial condition is given by Eq. 16. At the drying interface ($z = 0$), compression occurs in the z-direction due to a volume flux of liquid from the drying body into the bulk gas phase Q. Conservation of mass at $z = 0$ yields

$$\phi(0,t)Q + D(\phi(0,t))\left.\frac{\partial \phi}{\partial z}\right|_{(0,t)} = 0 \qquad t \ge 0 \tag{19}$$

while, at the bottom of the bed, there is no flux of particles and Eq. 18 holds. For drying systems, as long as the bed remains saturated, Q is found from the rate of mass transfer into the gas phase as

$$Q = k_g(p_v(\phi(0,t)) - p_a) \tag{20}$$

where k_g is the mass-transfer coefficient and $(p_v(\phi(0,t)) - p_a)$ is the difference between the vapor pressure at liquid-gas interface and in the bulk gas far away from the surface. In constant pressure filtration, Q is found from Eq. 15 for a given applied load. Alternately, if Q is specified as in drying, then the required compressive load is determined. Given the functions $P_y(\phi)$, $D(\phi)$, and Q, the evolution of the volume fraction profile $\phi(z,t)$ can be determined.

Following the formulation of Landman et al. (1991), Eq. 15 can be simplified by converting to a fixed boundary problem, as shown by Brown et al. (2002). The parameter $\overline{Q}$ defined by Brown et al. (2002) as

$$\overline{Q} = \frac{h_0 Q}{\phi_0 D(\phi_0)} = \frac{h_0 k_g(p_v(\phi_0) - p_a)}{\phi_0 D(\phi_0)} \tag{21}$$

where ϕ_0 is the initial volume fraction, h_0 is the initial bed height, k_g is the mass-transfer coefficient, p_v is the vapor pressure at the gas-liquid interface, and p_a is the ambient vapor pressure, gives a measure of the deformation behavior of the suspension during the consolidation phase of drying. When $\overline{Q} \ll 1$, the resistance to mass transfer occurs in the gas phase with the result that the suspension deforms and releases fluid such that an almost uniform volume fraction profile is maintained in the bed. For $\overline{Q} \gg 1$, large pressure gradients are required to express fluid at the gas/suspension interface resulting in significant volume fraction gradients. Changes to $\overline{Q}$ can be achieved by altering the interparticle bond strength through $P_y(\phi)$, the thickness of the samples, or the rate of evaporation.

Liquid in the pores between the particles at the saturated body/gas interface will have a chemical potential set by its being in equilibrium with the vapor just into the gas phase (that is, at $z = 0^-$). This chemical potential is lower than that of pure water at the same temperature and pressure, and results in a fluid pressure lower than atmospheric. Writing $P_l = P_{\text{atm}} + P_{\text{cap}}$ and noting that $P_{\text{app}} = P_{\text{atm}}$, we find from the force balances at all times in the saturated body $P_s + P_{\text{cap}} = 0$. As the capillary pressure P_{cap} is negative, $P_s > 0$, which, in our sign convention, means the solid phase feels a compressive or consolidating stress. We find P_{cap} through the use of the compressive yield stress constitutive equation which states that the characteristic time for particle rearrangement is small relative to the rate of drying such that $P_s(\phi(0,t)) = P_y(\phi(0,t))$, and, thus, $P_{\text{cap}}(t) = -P_y[\phi(0,t)]$. The vapor pressure is then found from the Kelvin equation

$$p_v = p_0 \exp\left(\frac{P_{\text{cap}} V_m}{R_g T}\right) \tag{22}$$

where p_0 is the vapor pressure that would exist if the interface were flat, V_m is the molar volume of the liquid, R_g is the gas constant, and T is the absolute temperature. By knowing $\phi(0,t)$, we find $P_y[\phi(0,t)]$ which can in turn be used to find p_v and, thus, through Eq. 20, Q.

If the saturated body had a uniform volume fraction and was allowed to equilibrate with the gas phase, the liquid vapor pressure would be set by Eq. 22 with $P_{\text{cap}} = P_{\text{cap}}^{\max}$ (White, 1982) where

$$P_{\text{cap}}^{\max}(\phi) \approx \frac{-3\gamma\phi}{(1-\phi)a_p} \tag{23}$$

Here γ is the liquid-vapor surface tension. The characteristic particle size a_p is derived as the inverse of the particle surface area per unit volume of suspension. If the particles are spheres packed in a relatively uniform manner, a_p will be the particle radius. However, for aggregated slurries with nonuniform microstructures composed of particles with nonspherical shapes and potentially wide size distributions, the value of a_p is difficult to ascertain.

As mentioned in the introduction, while $P_y(\phi(0,t)) < -P_{cap}(\phi(0,t))$, the volume fraction at $z = 0$ responds to evaporation by increasing (that is, the bed consolidates). At a drying time t_e, the condition $P_{cap}(t_e) = P_{cap}^{max}$ is met. Again, because we are using the compressive yield stress constitutive equation, this condition sets $\phi_e = \phi(0,t_e)$ and the volume fraction at $z = 0$ remains fixed for $t > t_e$. Further evaporation can only occur by desaturation of the bed. The time, t_e is easily determined in our experiments as the transition from a glossy to a matte finish and appears to coincide with the occurrence of cracks in the drying body. For conditions under which $\overline{Q} \ll 1$, the entire bed will be at a volume fraction of ϕ_e at time t_e. Note that while t_e changes with k_g, ϕ_e will be independent of k_g. For $t > t_e$, the rate of mass transfer into the gas phase will depend on mass-transfer resistances within the partially saturated bed. In this article, we focus on drying at times $t \le t_e$.

Previous descriptions of drying in saturated suspensions of particles include the treatment by Shishido et al. (1989) that considers osmotic pressure gradients as the driving force for moisture transfer. The approach by Scherer (1990) considers the driving force for shrinkage in gels during drying as being a combination of capillary pressure, osmotic pressure, disjoining pressure, and moisture stress. Our treatment differs from these in that the compressive strength and permeability of the suspensions are treated as functions of volume fractions independent of the drying process. The sensitivity of $P_y(\phi)$ to particle interaction forces ensures that the model incorporates these effects in predictions of the kinetics of the drying process. Also, in an approach similar to that of Smith et al. (1995), we are able to predict the volume fraction at which the suspension begins to desaturate. We apply below the models developed above to drying by characterizing $P_y(\phi)$ and $D(\phi)$ using the constant pressure filtration. The approximations developed by Landman et al. (1999) based on Eq. 12 are tested by comparing actual $H(t)$ data with model predictions requiring a knowledge of the full volume fraction dependence of $P_y(\phi)$ and $D(\phi)$ from ϕ_0 to ϕ_∞. Having determined all necessary adjustable parameters, we then test the ability of the two-phase fluid model with the compressive yield stress constitutive equation to predict ϕ_e and $\phi(z,t)$ in one-dimensional (1-D) drying experiments.

Experimental Studies

Aqueous suspensions of AKP-15 α-alumina particles (Sumitomo Chemical America Inc.) with median particle diameter of 0.65 μm suspended in 0.1 M NH_4Cl at pH4 and pH9 were used in drying and pressure filtration experiments. The samples were prepared using stock solutions of 0.2 M HCl and 0.2 M NH_4OH with final pH adjustments made using concentrated HCl or NH_4OH. Samples were prepared with initial solid volume fractions of 0.25 or 0.40. In order to minimize the effects of structural differences between different suspension samples, each was subjected to high-speed shear using an IKA LABORTECHNIK T25 high-speed shear mixer for 420 s at 133 s^{-1}, 180 s at 158 s^{-1}, and 120 s at 225 s^{-1}. The initial shearing process is an essential step in reproducible sample preparation (Channell and Zukoski, 1997).

Note that the Al_2O_3 system was chosen and used at pH4 and pH9 because of the observed difference in the charge on the particles under these conditions (Velamakanni and Lange, 1991). At pH4, the particles are positively charged while pH9 corresponds to the isoelectric point. Under these conditions, aqueous suspensions of these particles can be therefore expected to exhibit differences in rheological behavior due to differences between the particle interaction forces in the suspensions.

Compressive yield stress

The compressive yield stress $P_y(\phi)$ was measured using the fixed speed technique of Green et al. (1996) in a Beckman J2-2M/E centrifuge equipped with a JS-13.1 swinging bucket rotor at speeds of 377 rad/s and 838 rad/s. Samples were placed in specially modified centrifuge tubes with flat bases and centrifuged at the desired speed until equilibrium was achieved, as defined by there being no further changes in sediment height over a period of several hours. At equilibrium, the suspension consists of a clear supernatant above a dense layer of sediment separated by a sharp interface. By carefully decanting the supernatant, sectioning the underlying sediment and weighing the resulting slices before and after drying at 130°C for 172,800 s, the local volume fraction profile and the compressive yield stress as a function of volume fraction can be determined using Eq. 4.

Compressive yield stresses were also determined using an Instron, Model 4502 (a screw driven mechanical testing device) in which a series of compressive loads was applied to the suspension via a piston contained in a 0.0254 m diameter and 0.01 m high cylindrical filtration cell. The fluid phase was allowed to filter through a semi-permeable membrane (0.45 μm cellulose nitrate, MILLIPORE) of negligible resistance thereby allowing consolidation of the suspension. The equilibrium volume fraction was then determined for each applied load by weighing the filter cake before and after drying in an oven for 172,800 s at 130°C. This data provided a second measure of the compressive yield stress.

Filtration diffusivity

Constant pressure filtration experiments were conducted with the Instron, Model 4502 and yielded dynamic suspension height as a function of time. As discussed in the previous section, this data is used to determine β and from β, $D(\phi)$ is estimated.

Drying experiments

Drying experiments were conducted by flowing nitrogen gas over the samples at 0.0005 m^3/s, controlled using an AALBORG GFC37 mass-flow controller (0–0.0005 m^3/s, 3,400 kPa maximum). Samples were dried in cylindrical glass cells of diameter 0.0305 m and 0.148 m in depth with the walls and base insulated. The mass of the samples was recorded as a function of drying time to determine drying rates. Volume fraction profiles were determined at the end of each experiment by carefully sectioning the samples and measuring the weight of each section before and after drying in an oven for 172,800 s at 130°C. In order to determine the value of the mass-transfer coefficient k_g at given gas flow rates, evaporation experiments were conducted using de-ionized water.

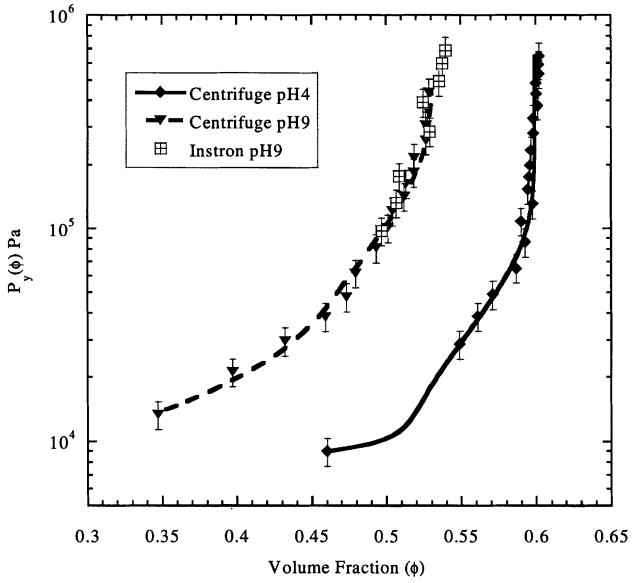

Figure 2. Compressive yield stress of AKP-15 Al_2O_3 suspended in 0.1 M NH_4Cl at pH4 and pH9 as a function of volume fraction determined using pressure filtration and centrifugation.

Fits shown are based on data in Table 1.

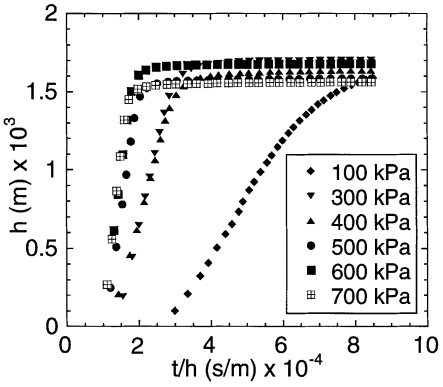

Figure 3. Volume per unit area (H) of the pressure filter as a function of t/H for various applied pressures in constant pressure filtration experiments on suspensions of AKP-15 Al_2O_3 particles in 0.1 M NH_4Cl at pH9.

Results and Discussion

Characterization of slurry properties

The compressive yield stress measured using pressure filtration and the centrifugal method are in good agreement, as shown in Figure 2. This result is consistent with previous studies (Green et al., 1996; Miller et al., 1996; Green and Boger, 1997) and indicated that independent experimental techniques yield the same values of $P_y(\phi)$. We choose to fit $P_y(\phi)$ data used in determining $D(\phi)$ and in simulations of pressure filtration and drying using

$$\phi = A_1\left[1 - A_2 \exp\left(-P_y/A_3\right)\right]\left[1 - A_4 \exp\left(-P_y/A_5\right)\right] \tag{24}$$

where A_i are constants. As shown in Figure 2, Eq. 24 captures the volume fraction dependence of $P_y(\phi)$ at both high and low volume fractions. The constants A_i are given in Table 1.

The compressive rheology of alumina suspensions has been extensively studied (Bergström et al., 1992; Channell and Zukoski, 1997; Landman et al., 1995; Miller et al., 1996; Valamcekanni and Lange, 1991). In agreement with these previous studies $P_y(\phi)$ measured here increases as the pH approaches the particle isoelectric point at a pH of 9. In our studies the background ionic strength was held to a minimum to reduce the risk of salt precipitation during consolidation. The compressive yield stress is sensitive to both pH and salt concentration reflecting changes in details in the strength of attraction at contact and possibly the slurry microstructure. Reproducibility of compressive yield stress results was ensured by high shear mixing during sample preparation.

Table 1. Coefficients Used in Eq. 24 for AKP-15 Al_2O_3 Particles Suspended in 0.1 M NH_4Cl at pH4 and pH9

Coefficient	pH4	pH9
A_1	0.60	0.53
A_2	1.02×10^{3}	1.09×10^{-1}
A_3 (Pa)	9.60×10^{2}	7.82×10^{3}
A_4	2.01×10^{-1}	2.27×10^{-1}
A_5 (Pa)	3.24×10^{4}	0.76×10^{5}

When constant pressure filtration experiments are conducted under conditions where the filter membrane resistance is low, Eq. 12 becomes valid and a plot of t/H as a function of H yields an approximate straight line of slope β^2. Here, t is the filtration time and H is the volume of filtrate expressed from the filter per unit filter cross section. Characteristic plots of t/H as a function of H for suspensions of AKP-15 Al_2O_3 particles in 0.1 M NH_4Cl at pH9 are shown in Figure 3 for several applied pressures. The short time behavior is well described by Eq. 12 at higher applied pressures and, to a lesser extent, at lower applied pressures. The discrepancy observed at lower applied pressures is thought to result from the bed being weak at the onset of filtration, as well as fluctuations in the applied pressure that become significant at these low pressures. Note that the height at which the suspension stops filtering determines the equilibrium volume fraction ϕ_∞. For all applied pressures, a value of β^2 was extracted by using a least-squares fit to the data, and the resulting values are shown in Figure 4. A similar plot of β^2 as a function of ϕ_∞ is shown in Figure 5 where discrete points in each plot represent experimental data and the corresponding solid line represents smooth curves through the data. We note that the nonlinearity of the curves in Figure 3 indicates the approximate form of Eq. 12. This results in some uncertainty in the resulting values of $D(\phi)$.

The β^2 values obtained from the filtration experiments along with the $P_y(\phi)$ data are used to determine the filtration diffusivity $D(\phi)$ or to obtain the hydrodynamic drag parameter $R(\phi)$ from Eqs. 13 and 14, respectively. Due to limitations with our filtration equipment, these experiments were conducted over a range of compressive loads that were larger than some of those experienced in the drying experiments. In

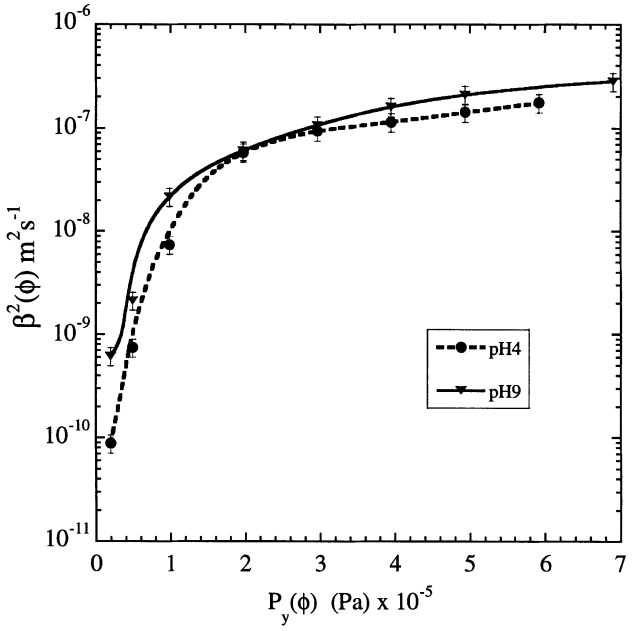

Figure 4. β^2 as a function of applied filtration pressure, $\Delta P = P_y$ for AKP-15 Al_2O_3 particles suspended in 0.1 M NH_4Cl at pH4 and pH9.

Lines are drawn to guide the eye.

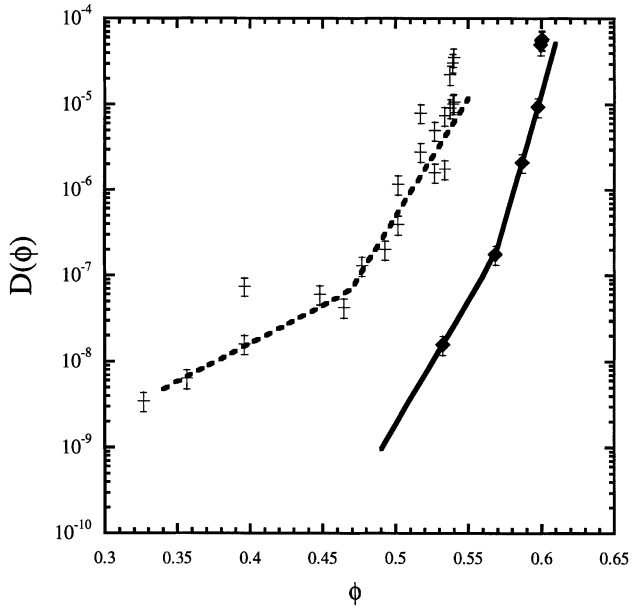

Figure 6. $D(\phi)$ as a function of volume fraction for AKP-15 Al_2O_3 suspended in 0.1 M NH_4Cl.

The crosses represent experimental values at pH9 and the diamonds represent experimental values at pH4. The lines represent fits using Eq. 25.

places where $D(\phi)$ data are needed outside the measured range, we rely on extrapolations in order to simulate both drying and pressure filtration.

The values of $D(\phi)$ in Figure 6 are based on the approximate links between β^2 and ΔP given in Eqs. 13 and 14. At both short and long times, $H(t)$ is not a linear function of $t^{1/2}$. As a consequence, $D(\phi)$ values shown are only approximate. Because prediction of $H(t)$ requires knowledge of $D(\phi)$ and $P_y(\phi)$ over the range ϕ_0 to ϕ_∞, a good test of the approximate methods used to find $D(\phi)$ can be obtained by predicting actual $H(t)$ data. Starting with approximate forms of $D(\phi)$ derived from β^2, one could iterate $D(\phi)$ values to match $H(t)$ for all ΔP. As a first step in such an iterative process, $H(t)$ was calculated using Eq. 24 for $P_y(\phi)$ and $D(\phi)$ calculated from

$$D(\phi) = B_{d1}\exp(C_{d1}\phi) \qquad \phi < \phi_1$$
$$D(\phi) = B_{d2}\exp(C_{d2}\phi) \qquad \phi \geq \phi_1 \qquad (25)$$

where B_{di} and C_{di} are constants given in Table 2.

As illustrated in Figure 7, model predictions compare well with experimental data over the entire filtration time even when the experimental data is not well fit by $H = \beta t^{1/2}$. From the comparisons in Figure 7, we conclude that our initial estimates of $D(\phi)$ are sufficiently accurate to capture the volume fraction dependence of filtration rates and further iterations are not required.

Under conditions consistent with those of our model system, values of $R(\phi)$ and hence $k(\phi)$ do not change significantly at low volume fraction. Indeed, the Carman-Kozeny

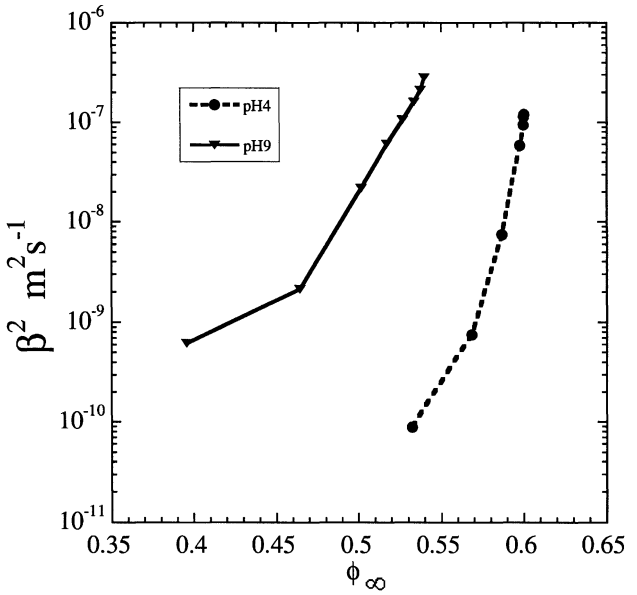

Figure 5. β^2 as a function of volume fraction for AKP-15 Al_2O_3 particles suspended in 0.1 M NH_4Cl at pH4 and pH9.

Lines are drawn to guide the eye.

Table 2. Coefficients Used in Eq. 25 for AKP-15 Al_2O_3 Particles Suspended in 0.1 M NH_4Cl at pH4 and pH9

Coefficient	pH4	pH9
B_{d1} (m^2/s)	5.4×10^{-11}	4.62×10^{-12}
C_{d1}	5.1	20.4
ϕ_1	0.484	0.467
B_{d2} (m^2/s)	2.18×10^{-41}	6.29×10^{-21}
C_{d2}	137.3	64.0

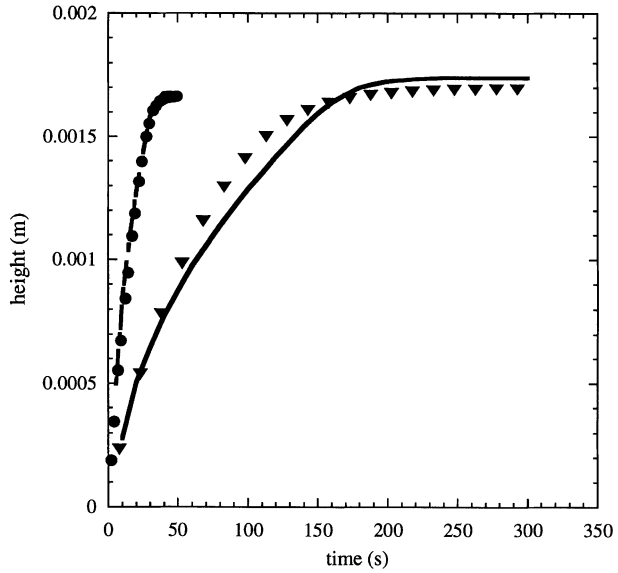

Figure 7. Measured vs. predicted piston heights at two different applied pressures for AKP-15 Al_2O_3 in 0.1 M NH_4Cl at pH9.

Circles: 600 kPa; triangles: 100 kPa.

equation for $k(\phi)$ ($k(\phi) = 0.022 a_p^2[(1-\phi)^3/\phi^2]$ is a poor representation of the experimental results even if a_p is taken as an adjustable parameter (Figure 8). As maximum packing is approached, values of $k(\phi)$ drop precipitously for both pH4 and pH9. As $k(\phi)$ is proportional to the ratio of $dP_y/d\phi$ to $D(\phi)$, both of which are changing rapidly as maximum packing is approached, small uncertainties in either quantity lead to large uncertainties in $k(\phi)$. We conclude that rather than assuming a form of $k(\phi)$ and using $P_y(\phi)$ data to predict $D(\phi)$, much more accurate predictions of pressure filtration kinetics are obtained by estimating $D(\phi)$ directly from β^2 data.

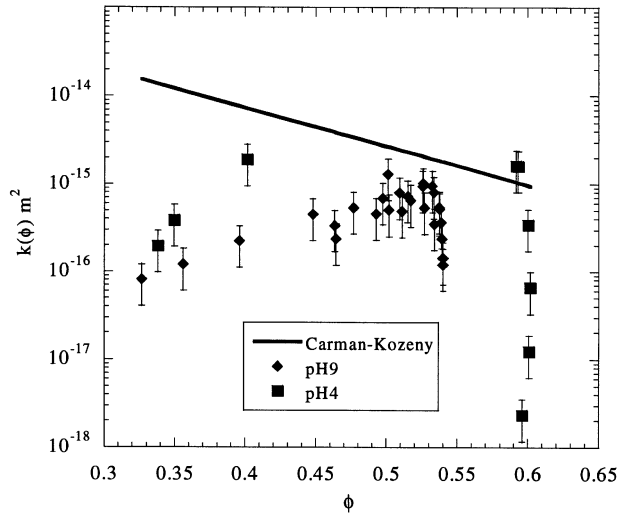

Figure 8. Permeability as a function of volume fraction for AKP-15 Al_2O_3 in 0.1 M NH_4Cl at pH4 and pH9.

The Carman-Kozeny lines are drawn with $a_p = 0.496$ μm.

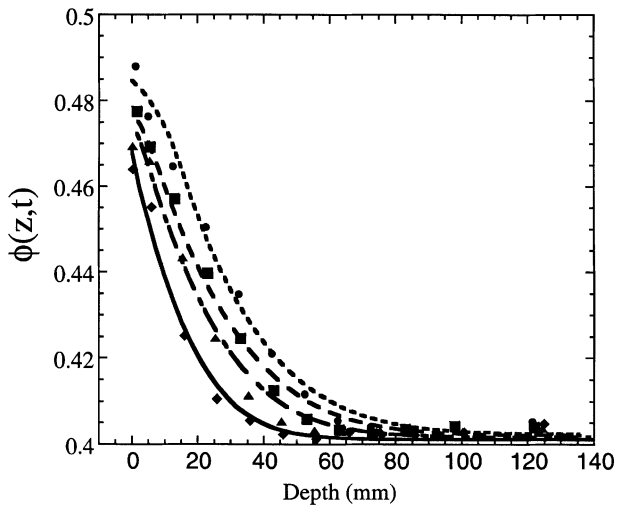

Figure 9. Volume fraction as a function of position in the bed at different drying times for a suspension of AKP-15 Al_2O_3 at pH9 in 0.1 m NH_4Cl.

Discrete points represent experimental data, while lines represent model predictions. From bottom to top drying times are 7,320 s, 13,980 s, 19,080 s, and 21,660 s.

The filtration diffusivity $D(\phi)$ is dominated by the volume fraction dependence of $P_y(\phi)$, and we again note that, as the suspension volume fraction is increased, estimation of $D(\phi)$ and $R(\phi)$ becomes increasingly difficult as small changes in volume fraction yield increasingly large changes in compressive yield stress. As a consequence, small experimental uncertainties result in large uncertainties in predictions of $D(\phi)$ from $R(\phi)$ or alternatively $R(\phi)$ from $D(\phi)$.

Application of $P_y(\phi)$ and $D(\phi)$ characterization to drying

Having characterized $P_y(\phi)$ and $D(\phi)$, and by knowing ϕ_0 and k_g, predictions of $\phi(z,t)$ can be made in drying slurries with no adjustable parameters. Figure 9 shows $\phi(z,t)$ for a pH9 sample with ($\phi_0 = 0.407$, $k_g = 7.3\times10^{-10}$ s·m^{2}kg^{-1}, $h_0 = 0.142$ m, $D(\phi_0) = 1.92\times10^{-8}$ m^{2}s^{-1}, $\overline{Q} = 3$). At a given time t, the volume fraction decays from a value of $\phi(0,t)$ towards ϕ_0 as one moves away from the interface, while $\phi(0,t)$ increases with time. The solid lines are model predictions made using $P_y(\phi)$ and $D(\phi)$ data derived from pressure filtration and centrifugation experiments. With no adjustable parameters, the predictions capture the behavior of $\phi(0,t)$, as well as the decay towards ϕ_0 at larger z.

As a demonstration of the role played by particle interaction forces in the drying consolidation, two suspensions, one at pH4 and the other at pH9 having identical dimensions (but different $P_y(\phi)$ and $D(\phi)$), were dried under similar conditions. Volume fraction profiles shown in Figure 10 were measured and compared with model predictions using $P_y(\phi)$ and $D(\phi)$ from Figures 2 and 7. While k_g was held constant at 7×10^{-10} s·m^{2}kg^{-1} for both experiments, $\overline{Q}$ was substantially different due to differences in $P_y(\phi)$ at the different pH values. For the suspension at pH4, ($\phi_0 = 0.335$, $h_0 = 0.138$ m, $D(\phi_0) = 2.98\times10^{-10}$m^2·s^{-1}, $\overline{Q} = 584$) while the suspension at pH9 has ($\phi_0 = 0.407$, $h_0 = 0.142$ m, $D(\phi_0) = 2.98\times10^{-10}$m^2·s$^{-1}\overline{Q} = 2.8$). Therefore, for the suspension at pH4, large volume fraction gradients develop, while at pH9 the

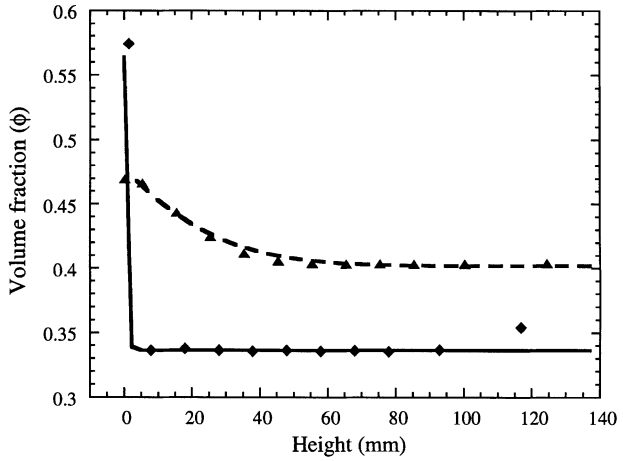

Figure 10. Evolution of volume fraction profile for AKP-15 Al_2O_3 in 0.1 m NH_4Cl at pH4 and pH9 under identical drying conditions.

Triangles and dashed line are experimental data and model predictions at pH9 at a time of 1.4×10^4 s. Diamonds and solid line are measures and predictions for pH4 at 1.5×10^3 s.

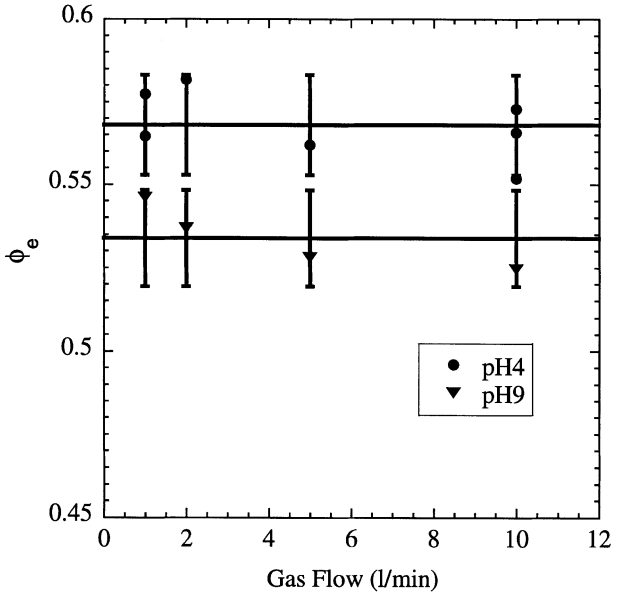

Figure 11. Experimentally determined volume fraction at which desaturation begins for AKP-15 Al_2O_3 particles suspended in 0.1 M NH_4Cl at pH4 and pH9.

The solid line is the average volume fraction in each case and the error bars represent one point five standard deviation from the mean taken over all flow rates. In these experiments $\phi_0 = 0.19$ (pH9), 0.23 (pH4), such that at t_e $\langle C(t_e)\rangle \cong 0.52$ M (0.47M) for pH9 (pH4).

suspension dries with a much more uniform volume fraction. Note that model predictions of $\phi(0,t)$, the gradient in ϕ, and the volume fraction far from the interface are well predicted by the model. The results in Figures 9 and 10 demonstrate that the two-phase fluid model incorporating the compressive yield stress constitutive equation provides an excellent description of the consolidation of aggregated, drying slurries.

In addition to being able to predict pressure filtration, $P_y(\phi)$ and $D(\phi)$ data also allows the drying consolidation model (Eqs. 15 to 19) to be solved numerically to provide estimates of ϕ_e and t_e. These parameters are found by matching the conditions that $P_y(\phi_e) = P_{\rm cap}^{\rm max}(\phi_e)$. While ϕ_e and t_e can be determined experimentally, like the permeability, calculating $P_{\rm cap}^{\rm max}$ from Eq. 23 is rife with uncertainties. However, the two-phase fluid model predicts that ϕ_e should be independent of k_g, and it follows naturally that t_e will decrease as k_g increases. As shown in Figure 11 for two suspensions initially at $\phi_0 = 0.23$ (pH4) $\phi_0 = 0.19$ (pH9), these expectations are met experimentally. On the other hand if ϕ_e is predicted from measured values of $P_y(\phi)$ and Eq. 23 with $a_p = 0.65$ μm and $\gamma = 0.072$ J·m^{-3}, ϕ_e is overestimated in some cases and underestimated in others. Reasons for the inability of Eq. 23 to predict ϕ_e include the effects of a broad particle-size distribution and the heterogeneous packing of the particles.

In addition, ϕ_e may not be well predicted by Eq. 23 because of the changing pore solution conditions during drying. For the slurries studied, P_y is a function of both ionic strength and pH, both of which may change in the pore fluid during drying. If the salt concentration is C_0 at the beginning of the drying experiment, at drying time t during consolidation, the average salt concentration in the pore fluid $\langle C(t)\rangle$ will be increased to $\langle C(t)\rangle = C_0\phi(1-\phi_0)/\phi_0(1-\phi)$. When $\overline{Q} \ll 1$, the volume fraction profile will be uniform in the bed, and, for our samples, the diffusion time for ions is much smaller than the rate of consolidation suggesting the ionic strength will increase uniformly in the consolidating slurry. If conditions are used where $P_y(\phi)$ is very sensitive to $\langle C(t)\rangle$, $P_y(\phi)$ will increase over the course of drying resulting in stiffer beds and a decrease in ϕ_e from the value of $P_y(\phi_e) = P_{\rm cap}^{\rm max}(\phi_e)$ where $P_y(\phi)$ is measured in pressure filtration or centrifugation at $\langle C\rangle = C_0$. This behavior is illustrated in Figure 12 showing experimentally measured values of $P_y(\phi)$ for suspensions of Al_2O_3 particles in 0.1M NH_4Cl at pH4 and pH9 under the conditions at the start of drying and at $\phi = \phi_e$ determined in Figure 11. Note that the impact of the changing solution is not the same in both cases. Indeed, for pH9, $P_y(\phi)$ at $\langle C(\phi_e)\rangle$ is smaller than $P_y(\phi)$ at $\langle C(\phi_0)\rangle$, while at pH4 the suspension has a larger compressive yield stress at the elevated volume fraction. On an absolute scale, these changes are relatively small. However, they are measurable. If $P_{\rm cap}^{\rm max}(\phi_e)$ is predicted from Eq. 23 with $\gamma = 7.2\times10^{-2}$ J·m^{-2} and at $a_p = 0.496$ μm, at pH9 ϕ_e is predicted to be ~ 0.53, from $P_y(\phi)$ measured at the initial ionic strength, while ϕ_e is predicted to be ~ 0.54 at ionic strengths which exist on average in the pore fluid at t_e. On the other hand, at pH4, ϕ_e is predicted to decrease ~ 0.015 volume fraction units due to bed stiffening during drying. The range of ϕ_e values shown in Figure 12 suggests stiffening at pH4 but mild reduction in $P_y(\phi)$ at pH9.

The data in Figures 11–12 highlight the sensitivity of the transition point to the strength of interactions and also the impact of changes in solution chemistry as drying progresses. Depending on the initial volume fraction, the solution conditions in the pores, the size of the drying object, and the particle surface chemistry, the bed may or may not stiffen appreciably during drying. In addition, if the salt concentration

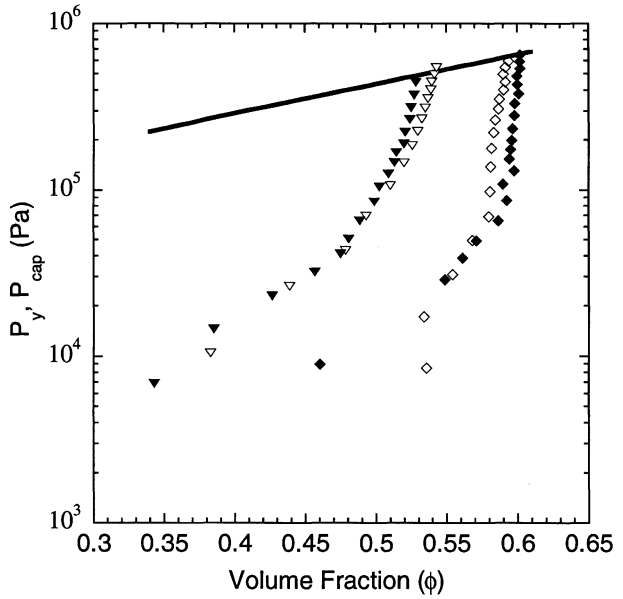

Figure 12. Compressive yield stress of AKP-15 Al_2O_3 in 0.1 M NH_4Cl at pH4 and pH9 under conditions at the start of drying (ϕ_0) and at the transition point (ϕ_e) given in Figure 11.

Closed triangles (pH9) and diamonds (pH4) represent $P_y(\phi)$ data measured at ionic strength conditions of 0.1 M NH_4Cl. The open triangles (open diamonds) correspond to $P_y(\phi)$ data measured for average ionic strength conditions corresponding to those given in Figure 11. The solid line is an approximation of $P_{cap}^{max}(\phi)$ calculated from Eq. 25 with $\gamma = 7.2 \times 10^{-3}$ Jm^{-2} and $a_p = 0.496$ μm.

reaches the solubility point, salt crystals can form with the effects of both reducing the rate of mass transfer and increasing the network strength (Guo and Lewis, 1999). Note that the success of the drying consolidation model in predicting $\phi(z, t)$ in Figures 9 and 10 results from the choice of experimental conditions where $\langle C(t_{max})\rangle/C_0 \cong 1$ and due to choice of experimental conditions where $P_y(\phi)$ is not overly sensitive to changes in $\langle C(t)\rangle$.

Conclusions

The two-phase fluid models used here for describing pressure filtration require knowledge of the compressive yield stress $P_y(\phi)$ and of the filtration diffusivity $D(\phi)$, both of which are strong functions of the solids volume fraction. In addition P_{cap}^{max} is required to determine the beginning of the desaturation period in drying. Due to the sensitivity of capillary pressure and permeability to details of the microstructure, these parameters are best characterized experimentally rather than using model calculations to determine their values.

We demonstrate here the ability of the compressive yield stress constitutive equation to describe dynamic suspension consolidation. This is accomplished by experimentally obtaining all necessary parameters using pressure filtration to characterize $P_y(\phi)$ and $D(\phi)$, then using this data to predict $H(t)$ in pressure filtration, the volume fraction where beds begin to desaturate in drying and changes in volume fraction profiles in drying beds with time. The excellent agreement observed between model predictions and experimental results demonstrates two central results. First, for stiff and brittle aggregated slurries, the compressive yield stress constitutive equation captures much of the underlying mechanics of consolidation in aggregated slurries. Secondly, the drying model of Brown et al. (2002) captures the details of the early stages of drying of aggregated slurries. We conclude that dimensional changes and volume fraction profiles in drying slurries can be manipulated through alteration in interparticle forces. Thus, an understanding of how solution conditions alter $P_y(\phi)$ and $D(\phi)$ provides a useful method for characterizing rates of consolidation, final volume fractions, and dimensional changes during drying.

Acknowledgments

The authors acknowledge support from the U.S. DOE via the University of Illinois at Urbana-Champaign, Frederick Seitz Materials Research Laboratory, Grant No. DEFG02-96ER45439. We would also like to thank Prof. Lee R. White for stimulating discussion throughout this research effort.

Literature Cited

Auzerais, F. M., R. Jackson, and W. B. Russel, "The Resolution of Shocks and the Effects of Compressible Sediments in Transient Settling," *J. Fluid Mech.,* **195**, 437 (1988).

Bergström, L., C. H. Schilling, and I. Aksay, "Consolidation Behavior of Flocculated Alumina Suspensions," *J. Amer. Ceram. Soc.,* **75**, 3305 (1992).

Brown, L. A., C. F. Zukoski, and L. R. White, "Consolidation During Drying of Aggregated Suspensions," *AIChE J.*, **48**, 492 (2002).

Buscall, R., and I. J. McGowan, "Sedimentation and Viscous Flow of a Weakly Flocculated Concentrated Dispersion," *Faraday Discuss. Chem. Soc.,* **76**, 277 (1983).

Buscall, R., and L. R. White, "The Consolidation of Concentrated Suspensions: 1. The Theory of Sedimentation," *J. Chem. Soc., Faraday Trans. 1*, **83**, 873 (1987).

Channell, G. M., and C. F. Zukoski, "Shear and Compressive Rheology of Aggregated Alumina Suspensions," *AIChE J.*, **43**, 1700 (1997).

Green, M. D., and D. V. Boger, "Yielding of Suspensions in Compression," *Ind. Eng. Chem. Res.*, **36**, 4984 (1997).

Green, M. D., M. Eberl, and K. A. Landman, "Compressive Yield Stress of Flocculated Suspensions: Determination via Experiment," *AIChE J.*, **42**, 2308 (1996).

Guo, J. J., and J. A. Lewis, "Aggregation Effects on the Compressive Flow Properties and Drying Behavior of Colloidal Silica Suspensions," *J. Amer. Ceram. Soc.,* **82**, 2345 (1999).

Landman, K. A., and W. B. Russel, "Filtration at Large Pressures for Strongly Flocculated Suspensions," *Phys. Fluids A*, **5**, 550 (1993).

Landman, K. A., C. Sirakoff, and L. R. White, "De-watering of Flocculated Suspensions by Pressure Filtration," *Phys. Fluids A,* **3**, 1495 (1991).

Landman, K. A., J. M. Stankovich, and L. R. White, "The Measurement of the Filtration Diffusivity $D(\phi)$ of a Flocculated Suspension," *AIChE J.*, **45**, 1875 (1999).

Landman, K. A., L. R. White, and R. Buscall, "The Continuous-Flow Gravity Thickener: Steady State Behavior," *AIChE J.*, **34**, 239 (1988).

Landman, K. A., and L. R. White, "Determination of the Hindered Settling Factor for Flocculated Suspensions," *AIChE J.*, **38**, 184 (1992).

Landman, K. A., and L. R. White, "Solid/liquid Separation of Flocculated Suspensions," *Systems & Computers in Japan*, **25**, 175 (1994).

Landman, K. A., L. R. White, and M. Eberl, "Pressure Filtration of Flocculated Suspensions," *AIChE J.,* **41**, 1687 (1995).

Miller, K. T., R. M. Melant, and C. F. Zukoski, "Comparison of the Compressive Yield Response of Aggregated Suspensions: Pressure Filtration, Centrifugation, and Osmotic Consolidation," *J. Amer. Ceram. Soc.,* **79**, 2545 (1996).

Scherer, G. W., "Theory of Drying," *J. Amer. Ceram. Soc.* **73**, 3 (1990).
Sherwood, J. D., "Initial and Final Stages of Compressible Filtercake Compaction," *AIChE J.*, **43**, 1488 (1997).
Sherwood, J. D., and G. H. Meeten, "The Filtration Properties of Compressible Mud Filtercakes," *J. Pet. Sci. and Eng.,* **18**, 73 (1997).
Shishido, I., T. Muramatsu, and S. Ohtani, "Local Moisture Content and Stress Distributions within Clay during Drying Shrinkage," *Heat Trans.-Jap. Res.,* **18**, 20 (1989).
Smith, D. M., G. W. Scherer, and J. M. Anderson, "Shrinkage during Drying of Silica Gel," *J. Non-Cryst. Solids,* **188**, 191 (1995).
Tiller, F. M., and B. Hsyung, "Unifying the Theory of Thickening, Filtration and Sedimentation," *Water Sci. and Tech.*, **28**, 1 (1993).
Usher, S. P., R. G. De Kretser, and P. J. Scales, "Validation of a New Filtration Technique for Dewaterability Characterization," *AIChE J.*, **47**, 1561 (2001).
White, L. R., "Capillary Rise in Powders," *J. Colloid Interface Sci.,* **90**, 536 (1982).
Velamcekanni, B. V., and F. F. Lange, "Effect of Interparticle Potentials and Sedimentation on Particle Packing Density of Bimodal Particle Distributions During Pressure Filtration," *J. Amer. Ceram. Soc.,* **74**, 166 (1991).
Yoon, S. J., "Volume Fraction Profile Evolution of Weakly Flocculated Suspension During Pressure Filtration," MS Thesis, University of Illinois at Urbana-Champaign (2000).

Manuscript received Mar. 15, 2002, and revision received July 18, 2002.